VOLUME 30 NUMBER 4 October 2024
pISSN 2287-2728
eISSN 2387-285X

CLINICAL and MOLECULAR HEPATOLOGY

The forum for latest knowledge of hepatobiliary diseases

T-cell therapy for HBV-HCC

Mortality from HCC and biliary tract cancers
Liver fibrosis scores and viral load in CHB
Genomic biomarkers for atezolizumab+bevacizumab in HCC
Epigenetic alteration of complement genes in MASLD

KASL

pISSN 2287-2728
eISSN 2287-285X

CLINICAL and MOLECULAR HEPATOLOGY

https://doi.org/10.3350/cmh.2024.0058
Clinical and Molecular Hepatology 2024;30:735-755

Original Article

Genetically-modified, redirected T cells target hepatitis B surface antigen-positive hepatocytes and hepatocellular carcinoma lesions in a clinical setting

Xueshuai Wan[1], Karin Wisskirchen[2], Tao Jin[2], Lu Yang[2], Xiaorui Wang[2], Xiang'an Wu[1], Fang Liu[1], Yu Wu[1], Christy Ma[2], Yong Pang[2], Qi Li[2], Ke Zhang[2], Ulrike Protzer[3], and Shunda Du[1]

[1]Department of Liver Surgery, Peking Union Medical College Hospital, PUMC, and Chinese Academy of Medical Sciences, Beijing, P. R. China; [2]SCG Cell Therapy Pte. Ltd., Singapore, Singapore ; [3]Institute of Virology, School of Medicine, Technical University of Munich/Helmholtz Munich, Munich, Germany

Graphical Abstract

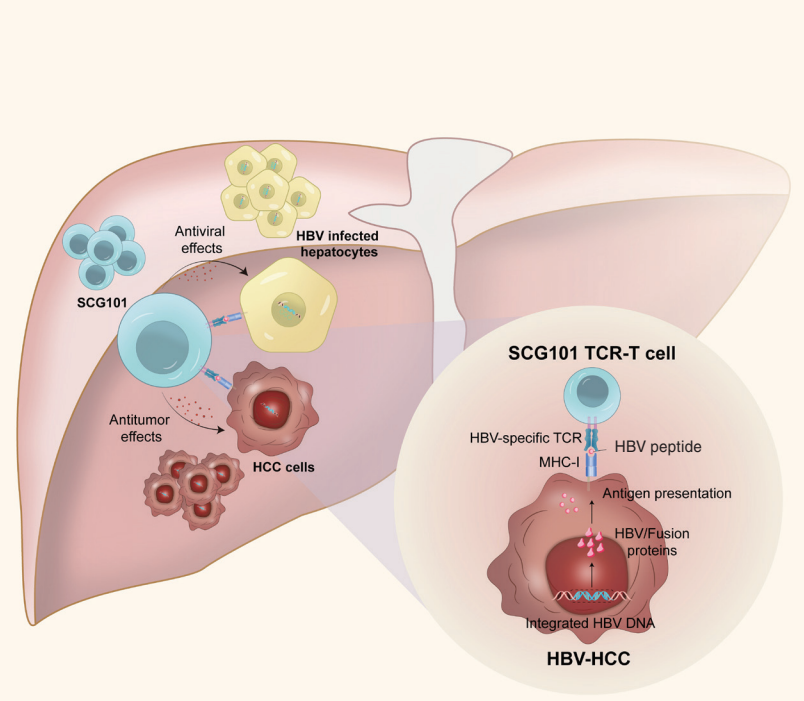

HBV-specific SCG101 TCR-T cells with verified efficacy and safety in preclinical and clinical settings confer dual functionalities against HBV-infected cells and HBV-HCC tumor cells.

Study Highlights

- Patient-derived T cells can be manufactured via lentiviral transduction under GMP conditions to express an HBV-specific TCR.
- HBV-specific T cells do not elicit off-target toxicity *in vitro*, *in vivo*, and in a patient suffering from an HBV-related HCC.
- HBV-specific T cells persist after single dosing in the HBV-HCC patient, resulting in robust HBsAg reduction and reduction of tumor lesions by >70%.

Copyright © 2024 by Korean Association for the Study of the Liver
This is an Open Access article distributed under the terms of the Creative Commons Attribution Non-Commercial License (http://creativecommons.org/licenses/by-nc/3.0/) which permits unrestricted non-commercial use, distribution, and reproduction in any medium, provided the original work is properly cited.

Background/Aims: Hepatitis B virus (HBV)-DNA integration in HBV-related hepatocellular carcinoma (HBV-HCC) can be targeted by HBV-specific T cells. SCG101 is an autologous, HBV-specific T-cell product expressing a T-cell receptor (TCR) after lentiviral transduction recognizing the envelope-derived peptide (S_{20-28}) on HLA-A2. We here validated its safety and efficacy preclinically and applied it to an HBV-related HCC patient (NCT05339321).

Methods: Good Manufacturing Practice-grade manufactured cells were assessed for off-target reactivity and functionality against hepatoma cells. Subsequently, a patient with advanced HBV-HCC (Child-Pugh class A, Barcelona Clinic Liver Cancer stage B, Eastern Cooperative Oncology Group performance status 0, hepatitis B e antigen-, serum hepatitis B surface antigen [HBsAg]+, HBsAg+ hepatocytes 10%) received 7.9×10^7 cells/kg after lymphodepletion. Safety, T-cell persistence, and antiviral and antitumor efficacy were evaluated.

Results: SCG101, produced at high numbers in a closed-bag system, showed HBV-specific functionality against HBV-HCC cells *in vitro* and *in vivo*. Clinically, treatment was well tolerated, and all adverse events, including transient hepatic damage, were reversible. On day 3, ALT levels increased to 1,404 U/L, and concurrently, serum HBsAg started decreasing by 3.84 $\log_{10}$ and remained <1 IU/mL for over six months. HBsAg-expressing hepatocytes in liver biopsies were undetectable after 73 days. The patient achieved a partial response according to modified RECIST with a >70% reduction in target lesion size. Transferred T cells expanded, developed a stem cell-like memory phenotype, and were still detectable after six months in the patient's blood.

Conclusions: SCG101 T-cell therapy showed encouraging efficacy and safety in preclinical models and in a patient with primary HBV-HCC and concomitant chronic hepatitis B with the capability to eliminate $HBsAg^+$ cells and achieve sustained tumor control after single dosing. **(Clin Mol Hepatol 2024;30:735-755)**

Keywords: Hepatitis B virus; Hepatocellular carcinoma; Immunotherapy; Cell therapy; T cell receptor

Corresponding author : Shunda Du
Department of Liver Surgery, Peking Union Medical College Hospital, Chinese Academy of Medical Sciences and Peking Union Medical College, 1 Shuaifuyuan, Wangfujing, Beijing 100730, P. R. China
Tel: +86-10-69152836, Fax: +86-10-69156043, E-mail: dushd@pumch.cn
https://orcid.org/0000-0002-9357-3259

Ulrike Protzer
Institute of Virology, Technical University of Munich/Helmholtz Munich, Trogerstrasse 30, 81675 Munich, Germany
Tel: +49-89-4140-6821, Fax: +49-89-4140-6823, E-mail: protzer@tum.de
https://orcid.org/0000-0002-9421-1911

Editor: Su Hyung Park, Korea Advanced Institute of Science and Technology (KAIST), Korea **Received :** Jan. 20, 2024 / **Revised :** May 28, 2024 / **Accepted :** May 28, 2024

Abbreviations:

ACT, adoptive cell therapy; AFP, alpha-fetoprotein; ALT, alanine aminotransferase; AST, aspartate aminotransferase; BCLC, barcelona clinic liver cancer; CAR, chimeric antigen receptor; CBA, cytometric bead array; CCR, C-C chemokine receptor; CD, cluster of differentiation; CHB, chronic hepatitis B; CNLC, China liver cancer; CRP, C-reactive protein; CRS, cytokine release syndrome; Cy/Flu, cyclophosphamide plus fludarabine; CT, computed tomography; DLT, dose-limiting toxicity; DNA, deoxyribonucleic acid; E:T, effector to target ratio; ECOG, eastern cooperative oncology group; GMP, good manufacturing practice; Gt, genotype; HBcAg, hepatitis B core antigen; HBeAg, hepatitis B e antigen; HBsAg, hepatitis B surface antigen; HBV, hepatitis B virus; HCC, hepatocellular carcinoma; HLA, human leukocyte antigen; IFN-γ, interferon-gamma; IL, interleukin; INR, international normalized ratio; iRECIST, immune Response Evaluation Criteria in Solid Tumors; LD, lymphodepletion; LHD, lactate dehydrogenase; MHC, major histocompatibility complex; mRECIST, modified Response Evaluation Criteria in Solid Tumors; NPG, NOD-Cg-PrkdcSCIDIL-2Rgcnull/vst; qPCR, quantitative polymerase chain reaction; RNA, ribonucleic acid; RTCA, real time cell analysis; SAE, serious adverse event; S20, amino acid position 20 of the HBV S protein; TCR, T cell receptor; TCR-T, T cell receptor T cells; TNF-α, tumor necrosis factor-α; TRAE, treatment related adverse event; ULN, upper limit of normal; UT, untransduced T cells

INTRODUCTION

Hepatocellular carcinoma (HCC) is the sixth most common malignancy and the third leading cause of cancer-related mortality worldwide.[1] Systemic HCC therapies encompass immune checkpoint, angiogenesis, or tyrosine kinase inhibitors, but response rates remain limited.[2] The risk of HCC recurrence is high because the therapies do not target the underlying cause of HCC development.

Hepatitis B virus (HBV) infection is the primary risk factor for HCC development, accounting for ~50% of HCC worldwide and ~85% in China.[3] Despite the implementation of vaccination programs, the projected number of liver cancer cases in China remains high, with 300,000 total cases predicted for 2030.[3] HBV-DNA integration is detected in 86% of HBV-related HCC tumor cells.[4] HBV-DNA integration contributes to tumorigenesis and can result in persistent expression of either complete hepatitis B surface antigen (HBsAg) or fragments thereof depending on the integration sites. This renders HBsAg an interesting therapeutic target as HBsAg is clearly distinct from proteins expressed in healthy liver tissue. As such, it represents an ideal target for adoptive cell therapy (ACT) of HBV-related HCC, as it is also able to address the underlying cause of HCC development. Clonal expansion of hepatocytes with HBV-DNA integration occurs early after infection and increases with disease progression.[5,6] Consequently, targeting these potentially premalignant cells seems crucial to prevent further HCC progression and the formation of new lesions.

HBV breakpoints resulting in HBV-DNA integration most commonly localize within a 1,800 bp region of the HBV genome, preserving the structural integrity of the envelope, X and polymerase open reading frames.[4] In advanced stages of chronic hepatitis B (CHB) and HCC, a substantial proportion of HBsAg appears to emanate from integrated DNA rather than from active viral infection,[7] and particularly ground glass hepatocytes contain abundant HBsAg.[8] The number of $HBsAg^+$ cells determined by histological staining is variable, ranging from 8–42% within tumor tissue and 71–86% in adjacent non-tumor tissue.[9-12] Even in histologically negative HCC samples, HBsAg RNA can be detected via qPCR and Nanostring technology.[13]

Immunopeptidomics analysis of HBV-HCC samples confirmed that most of the HBV peptides presented on tumor cells are derived from envelope and polymerase proteins[14,15] including the HBV peptide S_{20} (also referred to as Env_{183}) presented on human leukocyte antigen (HLA)-A*02.[14] T cells genetically modified to express HBV-specific TCRs can be redirected to recognize HBV-positive target cells.[16,17] Out of a library of HBV-specific TCRs, the most sensitive and highly specific, HLA-A*02-restricted TCR recognizing the HBV S_{20} peptide was selected for preclinical and clinical development.[17] T cells expressing this HBV-specific TCR secrete pro-inflammatory and antiviral cytokines, and selectively eliminate HBV-positive hepatoma cells and HBV-infected target cells, thereby clearing viral infection.[18]

In earlier clinical studies, T cells transiently expressing an HBV-specific TCR after RNA-electroporation were used to target HBV-HCC metastases.[13] In that setting, HLA-A2-restricted, HBV-specific T cells were repeatedly applied to patients that had been transplanted with an HLA-mismatched liver, thereby only targeting metastases of the original tumor but not the transplanted liver.[13] Given the mere mass of malignant cells within a solid tumor such as HCC, we hypothesized that tumor targeting and efficient killing of tumor cells would require a stable expression of an HBV-specific TCR to allow T cells to expand while maintaining their specificity and effector function. Therefore, a Good Manufacturing Practice (GMP)-compliant, semi-automated protocol for generating and upscaling an autologous T-cell product by lentiviral transduction and expansion was developed. Functionality and safety of the HBV-specific TCR T cell product (product code SCG101) were evaluated in preclinical models. Furthermore, for the first time, these stably TCR-expressing autologous cells were studied in a setting of primary HBV-related HCC and concomitant chronic hepatitis B. We here report the application of a single dose of SCG101 to an HLA-A*02:01-positive patient within an investigator-initiated clinical trial (NCT05339321).

MATERIALS AND METHODS

T-cell transduction

The patient's peripheral blood mononuclear cells were collected by leukocyte apheresis. Cells were sorted by magnetic beads carrying CD4 and CD8 antibodies (Miltenyi Biotec, Auburn, CA, USA) on a CliniMACS® Plus Instru-

ment under GMP conditions. Subsequently, the sorted $CD4^+$ and $CD8^+$ T cells were activated by TransAct microspheres presenting anti-CD3/CD28 antibodies (Miltenyi Biotec) and cultured in Prime-XV T-cell medium (Irvine Scientific, Santa Ana, CA, USA) with 400 IU/mL interleukin (IL)-2 (Shandong Quangang Co., Shandong, China).

A GMP-grade lentivirus (produced by WuXi AppTec. [Shanghai, China]) encoding the HBsAg-specific TCR gene was added to activated T cells on day 1. Cells were cultured at 37°C for 8 to 12 days in a closed bag system (Cytiva, Marlborough, MA, USA) on a Xuri Cell Expansion System W25 (Cytiva). Cells were harvested by 300×g centrifugation for 5 minutes at room temperature and then washed with a saline solution containing 5% human albumin (FLEXBUMIN; Baxter, Westlake Village, CA, USA). After washing, cells were frozen in CS10 medium (STEMCELL Technologies, Sunrise, FL, USA) and stored at –150°C.

T-cell functionality assays

For cytokine production assays, 5×10^4 T cells were co-cultured with an equal number of target cells in 96-well U-bottom plates. Reactivity against the HLA-A*02:01-presented S_{20} peptide was determined by pulsing T2 cells with peptide (1 μM, or as indicated) for two hours before co-culture. Co-culture supernatants were harvested after 18–24 hours, and interferon-gamma (IFN-γ), tumor necrosis factor-α (TNF-α), and interleukin-2 (IL-2) concentrations were measured by Cytometric Bead Array (CBA; BD Biosciences, San Jose, CA, USA) according to the manufacturer's instructions. Cytotoxicity assays were performed by co-culture of T cells with target cells at the indicated effector-to-target (E:T) ratios. Briefly, 2×10^4 target cells per well were seeded and cultured overnight before effector T cells were added at the indicated ratios. Target cell lysis was evaluated with the xCELLigence Real-Time Cell Analyzer (Agilent technologies, Santa Clara, CA, USA), which assessed electrical impedance due to the adherence of cells in each well every 15 minutes until the end of the experiment. The data were processed using the xCELLigence RTCA software, and the results were reported as a cell index value, which was set to 1 when T cells were added.

Patient characteristics and clinical intervention

The patient (code ST1206) described herein provided written informed consent to be enrolled in an investigator-initiated study (NCT05339321). The protocol was approved by the local ethics committee of the Peking Union Medical College Hospital. The study was conducted in accordance with the International Conference on Harmonization Guidelines for Good Clinical Practice and the Declaration of Helsinki. The patient received compensation for travel and a meal per visit. The primary objective of this study was to assess the safety and tolerability of SCG101 in HCC patients who were serum HBsAg positive, hepatitis B e antigen (HBeAg) negative, had HBV-DNA levels of $\leq2\times10^3$ IU/mL, were HLA-A*02 positive, and who had failed at least one prior line of treatment.

The enrolled participant presented here was HBeAg-negative individual with HBsAg level of 651 IU/mL during the screening phase. He was genotyped as HLA-A*02:01 and categorized as Child-Pugh A based on liver function assessment. Before intravenous infusion of SCG101, the patient received lymphodepletion chemotherapy (fludarabine 25 mg/m^2/day and cyclophosphamide 500 mg/m^2/day on days -6 to -4) for preconditioning. On day 0, the subject received 7.9×10^7 TCR-T cells per kg, corresponding to 5.9×10^9 total TCR-T cells. Cell infusion took 70 minutes.

Efficacy was evaluated according to modified Response Evaluation Criteria in Solid Tumors (mRECIST) and immune RECIST (iRECIST). Imaging and tumor assessment were conducted in month one, month two, and every two months thereafter, using contrast-enhanced computed tomography (CT).

Biopsy staining

Liver biopsies were formalin-fixed and paraffin-embedded before 4 μm tissue sections were obtained. Immunohistochemistry staining using the BOND RX Fully Automated Research Stainer (Leica, Wetzlar, Germany) with a bond polymer refine DAB detection. Deparaffinized slides were incubated with anti-HLA-A (#ab52922; Abcam, Cambridge, UK), anti-hepatitis B core antigen (HBcAg) (#CHM-0100; CELNOVTE, Zhengzhou, China) or anti-HBsAg (#CHM-0121; CELNOVTE) antibody for 60 minutes and then treated with anti-polymer peroxidase-conjugated

https://doi.org/10.3350/cmh.2024.0058

(HRP) secondary antibody (#DS9800; Leica) for 30 minutes. Slides were then treated with hematoxylin, washed in distilled water, counter-stained with eosin and manually covered. Slides were air-dried and mounted with an antifade mounting medium, and pictures were taken on a Pannoramic Midi II system (3DHistech Ltd.).

RESULTS

Specificity of the clinical T-cell product SCG101

SCG101 is a human TCR T-cell product expressing a natural, high-affinity TCR isolated from an HLA-A*02:01$^+$ donor with resolved HBV infection.[17] The TCR construct comprises V alpha 34 and V beta 5.1 variable domains fused to minimally-murinized cysteine-modified constant domains to enhance correct pairing of the TCR chains while keeping immunogenicity at a minimum (Fig. 1A).[19] The TCR was cloned into a lentiviral vector for transduction of T cells with a GMP-compliant protocol. As part of the cell product assessment before clinical application, SCG101 T cells were characterized *in vitro* and in preclinical models.

Specific binding of the TCR to its peptide-MHC complex (S_{20} FLLTRILTI_HLA-A*02:01) was dose-dependent with a half-maximum binding activity of 2.1 nM (Fig. 1B). Within primary SCG101 T cells, CD8$^+$ as well as CD4$^+$ T cells were able to bind the S_{20} multimer, indicating a transduction rate of almost 90% (Fig. 1C). Staining using an antibody specific to the human TCR variable beta chain 5.1 (TCRVβ5.1), and an HLA-A*02-S_{20} multimer allowed to estimate TCR expression and pairing efficiency, respectively. Accordingly, TCR mispairing with endogenous TCR sequences could be deduced from positive Vβ staining in the absence of multimer-binding. The maximum likelihood of such mispairing was low, with a mean value of 7% among six batches of SCG101 T cells (Fig. 1C).

To investigate the specific binding of SCG101 further, we aimed to assess critical amino acids within the TCR epitope sequence that are either essential for recognition by SCG101 T cells or for peptide binding to the HLA-A2 molecule. The exchange of L-T-R-I at position S22-S25 led to a 90–99% reduced recognition of the peptide, indicating the potential binding motif (Fig. 1D). Next, we assessed the cross-reactivity of SCG101 with human peptides and potential off-target activity. Neither the nine human peptides identified to contain the potential binding motif L-T-R-I (Fig. 1E, Supplementary Fig. 1A) nor the 14 peptides that shared six identical amino acids with peptide S_{20} (Fig. 1F, Supplementary Fig. 1B) led to activation of SCG101 T cells. Hence, the results demonstrated the specificity of SCG101's TCR and indicated the absence of cross-reactivity against tested very similar human peptides. Taken together, the SCG101 T-cell product exhibited clearly recognizable levels of TCR expression and correct TCR chain pairing while retaining specificity to its cognate HBV peptide.

Potency of SCG101 T cells

We next asked whether the clinical-grade SCG101 T cell product produced using a new upscaling protocol under GMP conditions would maintain antiviral and antitumor potency.[18] The functional avidity of SCG101 was measured by secretion of pro-inflammatory cytokines towards a dose-titration of peptide S_{20} loaded onto T2 cells compared to peptide C_{18}, which should not be recognized (Fig. 2A). IFN-γ secretion proved most sensitive with an EC_{50} of 1.55×10^{-8} M. When co-cultured with HBsAg$^+$ HepG2 hepatoma cells, SCG101 T cells were able to kill rapidly and specifically up to 100% of target cells within 48 hours (Fig. 2B). Consistent with the cytotoxic capability of SCG101, the antiviral cytokine IFN-γ was produced at high levels of 20 ng/mL upon antigen stimulation at an E:T of 1:1 (Fig. 2C). HBsAg in supernatants was also reduced by approximately 50% within two days of co-culture (Fig. 2D).

In vivo efficacy of SCG101 T cells

To analyze the anti-tumor activity and tissue distribution of SCG101 in an *in vivo* model, we used a xenograft model with transplanted HBsAg$^+$ hepatoma cells. When tumors had formed, four different SCG101 dose levels ranging from 2 to 20 million TCR$^+$ T cells were applied (Fig. 3A). Animals did not lose body weight during treatment (Fig. 3B), and by day 21, tumor growth inhibition in all SCG101 TCR-T groups was >95% (Fig. 3C).

The same preclinical model was also used to study the pharmacokinetics of the highest dose of TCR$^+$ T cells (Supplementary Fig. 2A). The distribution of SCG101 was ana-

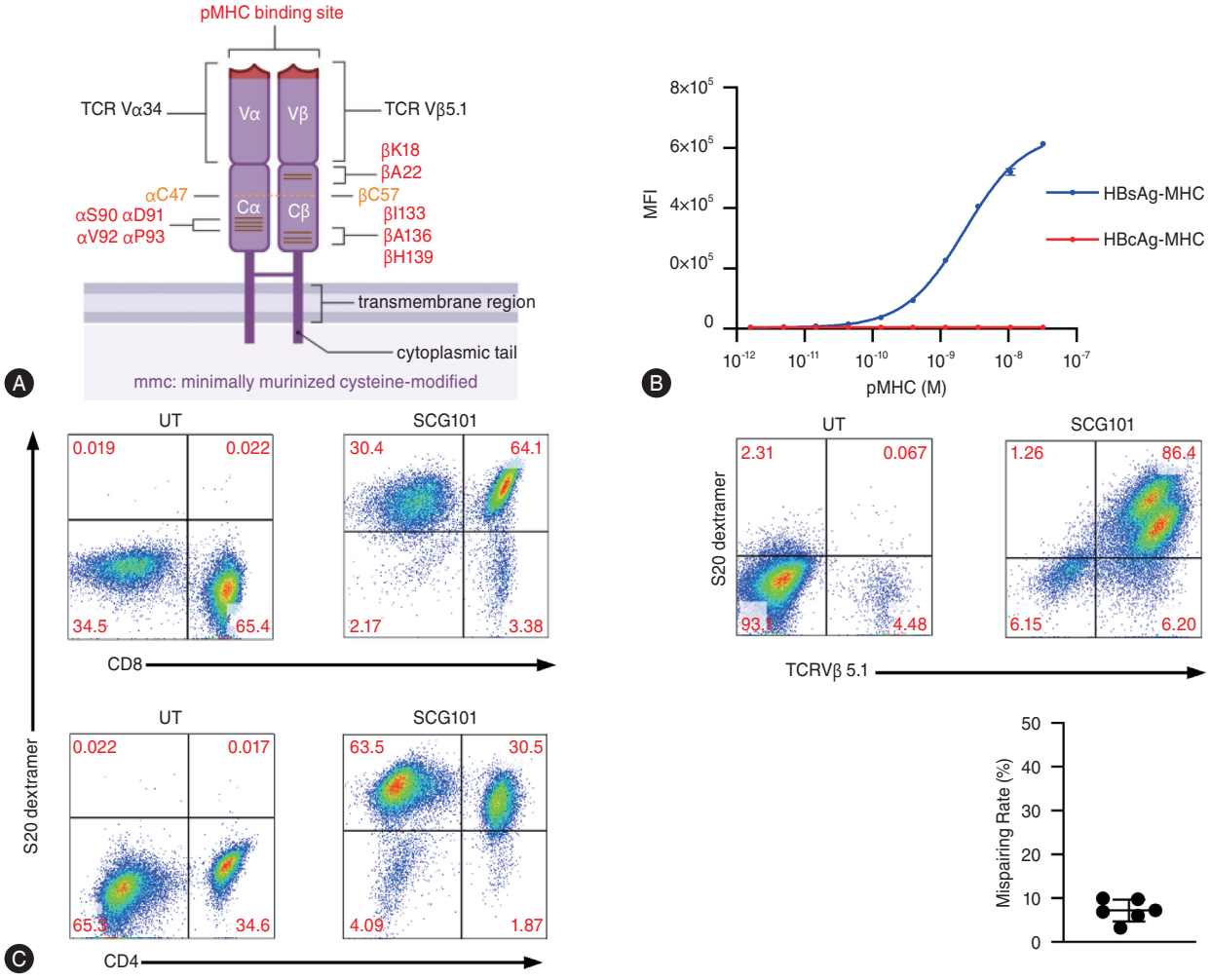

Figure 1. Properties of the clinical HBV-specific T cell product SCG101. (A) Schematic structure of the HLA-A*02-restricted, HBV S_{20}-specific T cell receptor (TCR) used for transduction of T cells to generate SCG101. To increase TCR expression and correct pairing, TCR chains were codon-optimized, and an additional cysteine bond (orange, dashed line) was introduced to the constant domains. The human constants harbored nine amino acids from the murine TCR constant domains as indicated (red lines). pMHC, complex of peptide and MHC. (B) Binding strengths of TCR SCG101 expressed in Jurkat cells. Jurkat-SCG101 were stained with decreasing amounts of HLA-A*02:01-S_{20} (FLLTRILTI)-PE-labeled multimers (blue circles) or with an HLA-A*02:01-C_{18} (FLPSDFFPSV) multimer (red circles) as negative control. The mean fluorescence intensity (MFI) was quantified by flow cytometry. (C) TCR expression in $CD8^+$ and $CD4^+$ T cells after lentiviral transduction was detected by co-staining S_{20} dextramer and anti-human CD4/CD8. The binding of a PE-labeled S_{20}-multimer indicates correctly paired TCR chains and Vβ5.1-FITC staining indicates the proportion of transduced T cells. Quantification of the potential TCR mispairing rate in % as a quotient of total S_{20} dextramer+ cells divided by (total $V\beta5.1^+$ cells – endogenously expressing $V\beta5.1^+$ cells). Mean±SEM for mispairing rates of six SCG101 batches are shown. Untransduced cells (UT) served as a control to quantify T cells endogenously expressing Vβ5.1. (D) Estimation of the SCG101 recognition motif by alanine scanning. Each native residue of peptide S_{20} (FLLTRILTI) was substituted at each position for an alanine. T2 cells were pulsed with 1 μM of each modified peptide indicated on the x-axis and co-cultured with SCG101 TCR-T, the IFN-γ concentration was measured by CBA. The prototype S_{20}-gtA/D and the C_{18} peptide were set as positive or negative controls, respectively. (E) Cross-reactivity screening of SCG101 against human peptides containing the core binding motif L3 / T4 / R5 / I6 at concentrations of 1 (blue circles) and 0.1 (red circles) μg/mL. (F) Cross-reactivity of SCG101 against human peptides containing ≥ six amino acid sites consistent with the S_{20} peptide. S_{20}-B/C peptide FLLTKILTI represents a variant often found in HBV genotypes B and C. Mean values of duplicates are shown. The labeling indicates the name of the human gene containing the respective peptide sequence. HBV, hepatitis B virus; HLA, human leukocyte antigen; SEM, standard error of the mean; IFN-γ, interferon-gamma; CBA, cytometric bead array.

lyzed by qPCR of 14 different tissues at six consecutive time points over three weeks. After a single dose of 1×10^9 TCR^+ T cells/kg, the cells had rapidly distributed throughout the body by day one. After a gradual decrease of SCG101 in all tissues by day seven, copy numbers increased again in the following two weeks, peaking on day 21 (Supplemen-

https://doi.org/10.3350/cmh.2024.0058

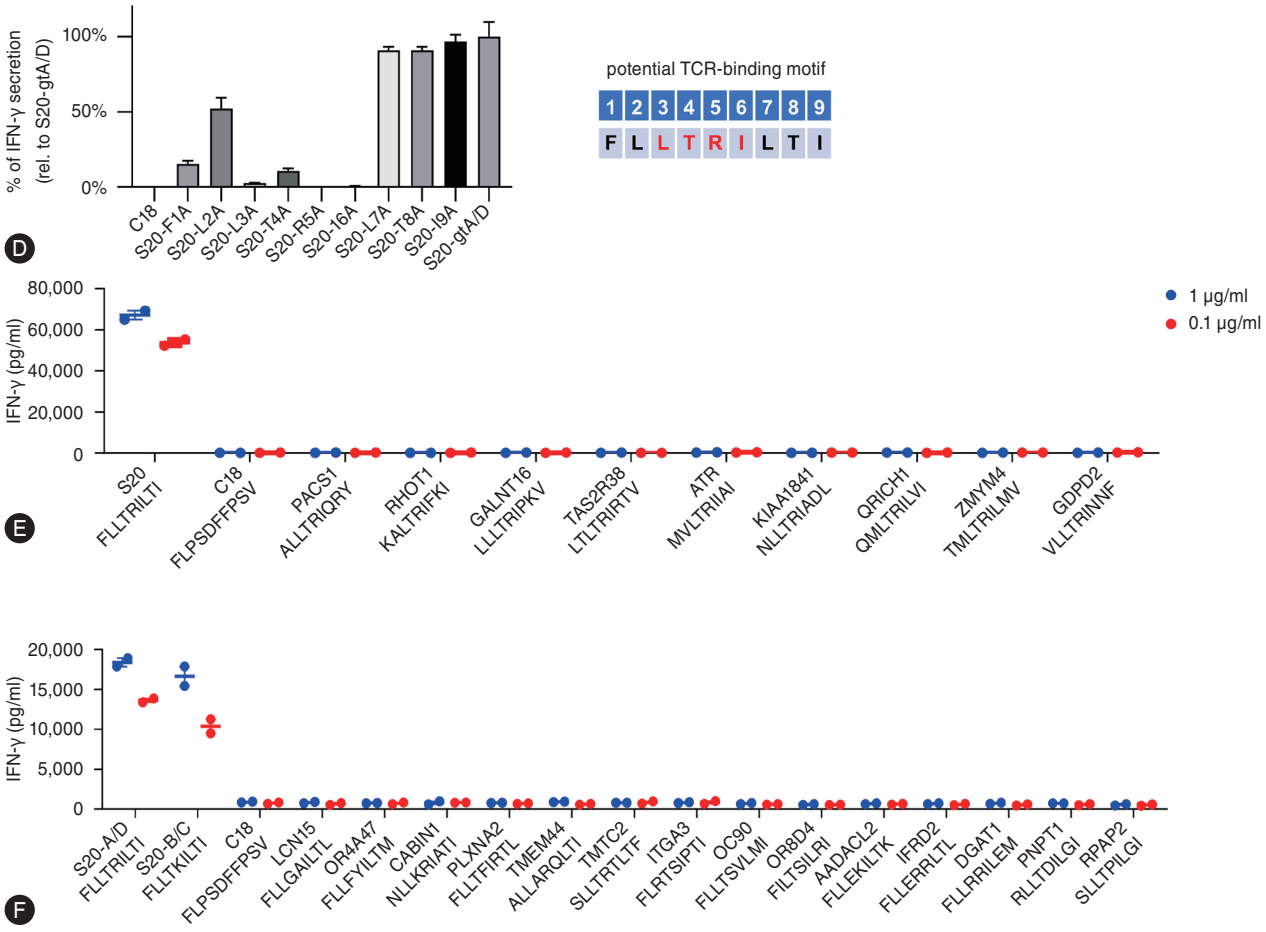

Figure 1. Continued.

tary Fig. 2B), indicating T-cell expansion upon antigen recognition. SCG101 accumulated mainly in the lung, spleen, blood, and liver (Supplementary Fig. 2C). Taken together, SCG101 TCR-T mediated a high target-specific anti-tumor activity and initiated T-cell persistence *in vivo*.

Application of HBV-specific T cells in a clinical setting

Encouraged by the preclinical data showing the anti-tumor activity of SCG101, an investigator-initiated trial, "Clinical study of SCG101 in the Treatment of Subjects with Hepatitis B Virus-Related Hepatocellular Carcinoma (SCG101-CI-101)", was set up. It was approved by the local ethics board. A 54-year-old HLA-A*02:01^{+} man diagnosed with CHB and HCC in 2019 was enrolled in the study and infused with SCG101 in July 2022. The patient had a history of tumor and liver segment VIII resection in 2019, followed by transarterial chemoembolization in 2019 and 2021 and sorafenib treatment for one year. The patient started to take entecavir for HBV infection management in March 2022 (Fig. 4A). The status of his liver disease was Child-Pugh class A, Eastern Cooperative Oncology Group (ECOG) performance status 0, BCLC stage B and China liver cancer (CNLC) classification stage IIb without extrahepatic metastasis, portal vein thrombosis, or other comorbidities (Fig. 4B).

An archived liver biopsy sample taken three months before adoptive T-cell transfer was analyzed (Fig. 4C). Despite having multiple nodules and two target lesions, obtaining tumor biopsy was unsuccessful. Histological analysis revealed an intense HLA-A staining along sinusoids and a weaker HLA-A staining on hepatocytes (Fig. 4D). The tissue stained negative for HBcAg (Fig. 4E) and

 https://doi.org/10.3350/cmh.2024.0058

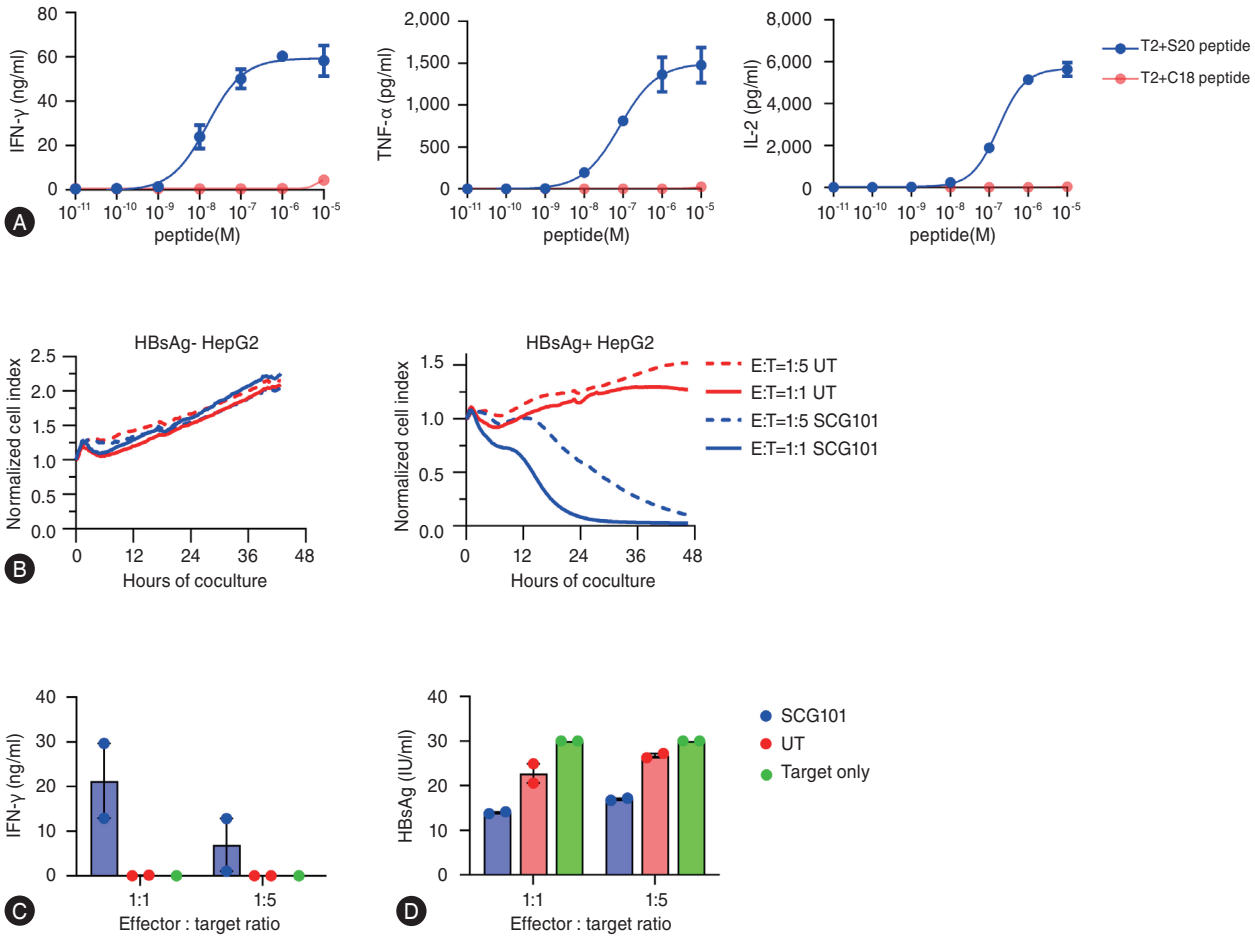

Figure 2. *In vitro* potency of the HBV-specific T-cell product SCG101. (A) The functional avidity of SCG101 T cells was assessed by titration of the S_{20} peptide (blue circles) loaded on T2 cells. The concentration of IFN-γ, TNF-α, and IL-2 in supernatants after 24 hours of co-culture was measured by CBA. C_{18} peptide (red circles) loading served as a negative control. (B) Cytolysis of tumor cell lines determined by the impedance of adherent target cells via xCELLigence real-time measurement. HBsAg negative (left) or positive (right) HepG2 target cells were co-cultured with SCG101 (blue lines) or untransduced (UT, red lines) at an effector-to-target (E:T) ratio of 1:1 (solid lines) or 1:5 (dashed lines). Mean values are shown. (C) Supernatants of the co-cultures were analyzed for IFN-γ after 48 hours by CBA. (D) HBsAg in supernatants after 48 hours of co-culture was measured by a quantitative ELISA. Data from two donors (C, D mean±SEM) are shown. HBV, hepatitis B virus; IFN-γ, interferon-gamma; TNF-α, tumor necrosis factor-α; IL, interleukin; HBsAg, hepatitis B surface antigen; SEM, standard error of the mean; CBA, cytometric bead array.

an average of around 10% of hepatocytes across three different sections stained positive for HBsAg (Fig. 4F).

After signing informed consent, the patient underwent leukapheresis to obtain peripheral blood mononuclear cells to produce SCG101 with the standardized protocol under GMP conditions. The cell product contained 30% TCR^+ T cells, with $CD8^+$ and $CD4^+$ T-cell frequencies of 62.12% and 36.78%, respectively (Supplementary Fig. 3A), and passed all the quality controls and release criteria (Supplementary Fig. 3B). The data cut-off was February 7, 2023.

Treatment-related events

One week before treatment, lymphodepletion was performed on three consecutive days using cyclophosphamide and fludarabine. Finally, a single dose of 7.9×10^7 per kg corresponding to 5.9×10^9 total TCR-T cells was infused. Upon adoptive T-cell transfer, the patient was closely monitored for treatment-related adverse events (TRAE) and blood was analyzed regularly (Fig. 5A). The patient tolerated SCG101 therapy well; no treatment-related serious adverse events (SAEs), neurotoxicity, or infusion reactions

https://doi.org/10.3350/cmh.2024.0058

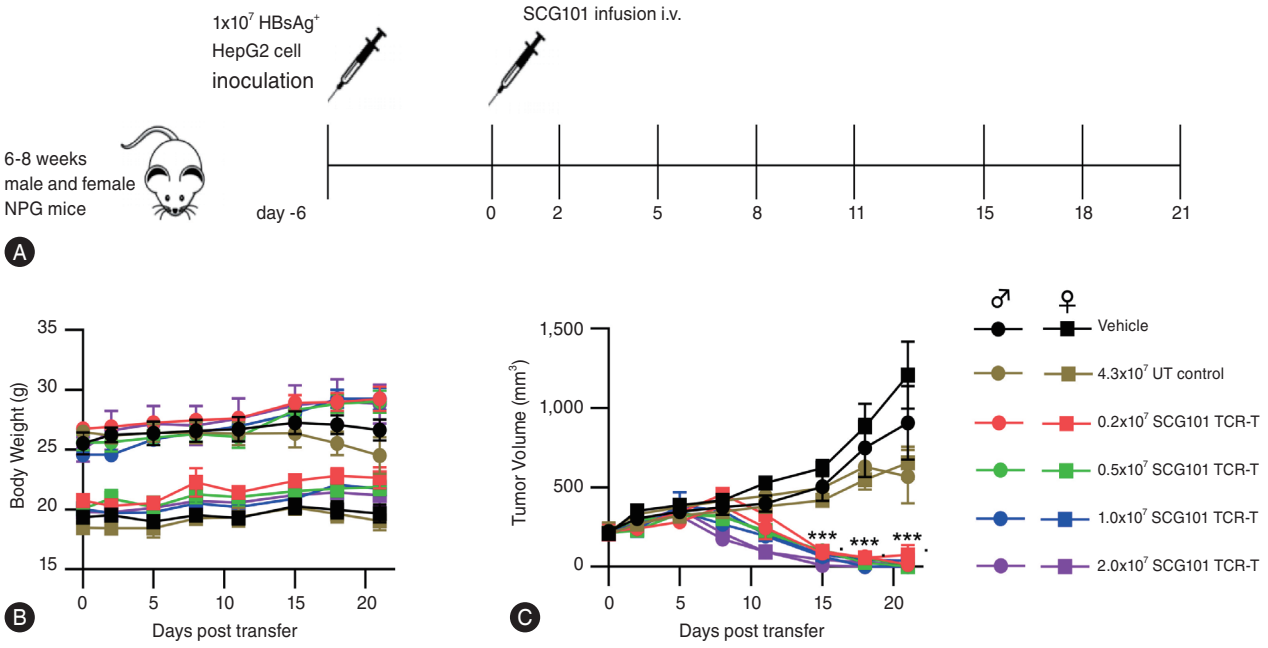

Figure 3. *In vivo* anti-tumor potency of HBV-specific SCG101 T cells. (A) NOD-Cg-PrkdcSCIDIL-2Rgcnull/vst (NPG) mice (female:male=1:1) were subcutaneously inoculated with 1×10^7 HBsAg$^+$ hepatoma cells/animal in the right armpit. After six days, 60 animals were divided into six groups. Mice received either increasing numbers of SCG101, multimer positive T cells of 0.2 to 2×10^7 TCR-T cells/animal, or a mixture of CS10, HSA, and sodium chloride (vehicle, black lines), or untransduced T cells (UT, 4.3×10^7 cells/animal, brown lines) according to the total number of T cells in the highest SCG101 group. Injections were done intravenously and (B) body weight and (C) tumor volume were analyzed twice weekly. Mean±SEM of n=10 per group, 5 males (circles) and 5 females (squares) are shown. HBV, hepatitis B virus; HBsAg, hepatitis B surface antigen; TCR-T, T cell receptor T cells; SEM, standard error of the mean. ***P≤0.001.

occurred and all TRAEs were manageable and reversible (Table 1, Supplementary Fig. 4). TRAEs of grade 3 or 4 included cytokine release syndrome (CRS), hypotension, cytopenia, alanine aminotransferase (ALT) and aspartate aminotransferase (AST) increase (Table 1). Cytopenia, which was anticipated due to the Cy/Flu preconditioning, comprised a decrease in lymphocytes, monocytes, neutrophils, and total white blood cells (Table 1, Supplementary Fig. 4A–D) and, in general, recovered to grade 2 within 30 days. However, a prolonged decrease and fluctuating platelet counts constituting grade 2 to grade 4 events were observed and finally resolved on day 80 (Supplementary Fig. 4E).

Since SCG101 can not only target the tumor but also infected hepatocytes, as observed in preclinical models,[18] particular attention was given to the liver function. Pretreatment ALT was 18 U/L, the pretreatment international normalized ratio (INR) for blood clotting was 1, and the pretreatment bilirubin level was 14.0 μmol/L. ALT elevation after SCG101 infusion reached a peak of 1,404 U/L on day 3 (Fig. 5B), that of AST 1,140 U/L on day 2 (Fig. 5C), respectively, both constituting grade 4 events (Table 1). After liver protection therapy, including glutathione, diammonium glycyrrhizinate, ademetionine, and polyene phosphatidylcholine, ALT, AST, and lactate dehydrogenase (Fig. 5D) levels decreased gradually.

Elevation of liver enzymes was transient, returned to baseline on day 17, and was accompanied by a slight, transient increase in serum total bilirubin below two times the upper limit of normal (ULN) (Fig. 5E, Supplementary Fig. 4G), ferritin (Fig. 5F), creatinine and urea (Supplementary Fig. 4H, I), as well as a reduction in serum albumin below 35 g/L on a single day (Fig. 5G), while the INR remained normal (Fig. 5H).

After infusion of SCG101, a strong immune reaction followed, characterized by C-reactive protein (CRP), IL-6, IFN-γ, IL-2, and IL-10 increasing rapidly one day after infusion (Fig. 5I–M, Supplementary Fig. 4J), temperature

 https://doi.org/10.3350/cmh.2024.0058

A

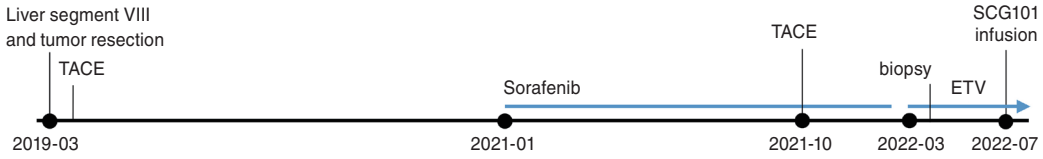

B

Age	Gender	HLA-A	HLA-B	HLA-C	Child-P.Score	ECOG status	BCLC status	CNLC status
54	male	*02:01 *23:01	*39:24 *44:03	*04:01 *07:01	A	0	B	IIb

C D E

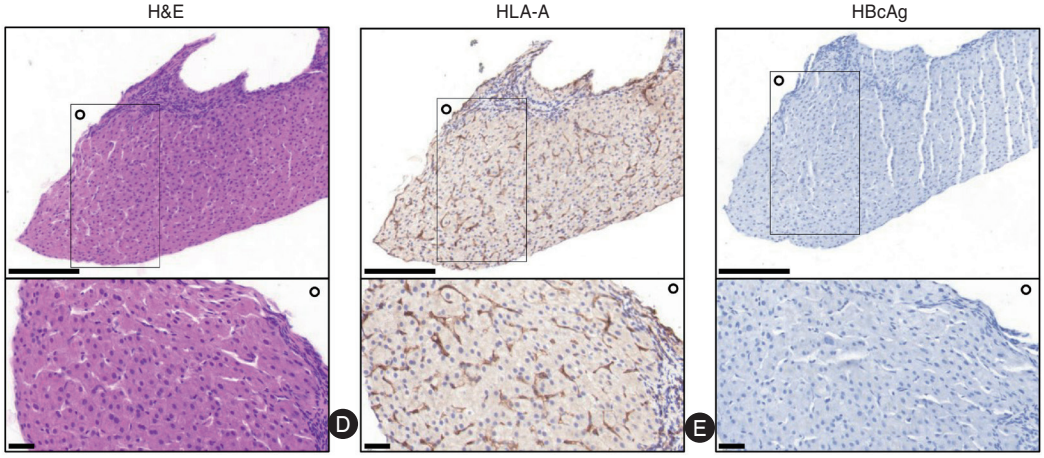

F

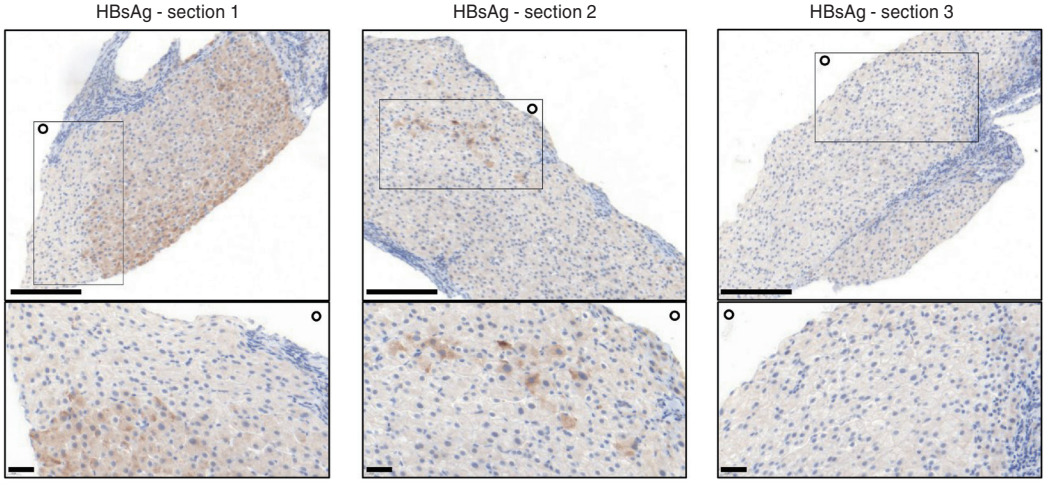

Figure 4. Patient characteristics. (A) Scheme of the medical history of HCC diagnosis and treatment of patient ST1206. Study enrollment was initiated after the failure of three prior HCC treatments (resection, transarterial chemoembolization [TACE] with Raltitrexed and Lobaplatin, and Sorafenib). (B) HLA profile and status of liver disease of patient ST1206 including Child-Pugh-Score, Eastern Co-operative Oncology Group (ECOG) performance status, Barcelona Clinic Liver Cancer (BCLC) staging, and China liver cancer (CNLC) classification. Blue lines indicate duration of systemic treatments. ETV=Entecavir. (C–F) Immunohistological analysis of a liver biopsy taken three months prior to treatment. Four pieces of non-tumor liver tissue were obtained, and representative sections are shown. Scale bars: 200 μm and 40 μm (inlay), respectively. The circle indicates the orientation of the inlay. (C) Morphological analysis using hematoxylin and eosin (H&E) staining. Immunostainings for (D) HLA-A, (E) HBcAg, and (F) HBsAg (three different sections are shown because of a diverse expression profile). HCC, hepatocellular carcinoma; HLA, human leukocyte antigen; HBcAg, hepatitis B core antigen; HBsAg, hepatitis B surface antigen.

https://doi.org/10.3350/cmh.2024.0058

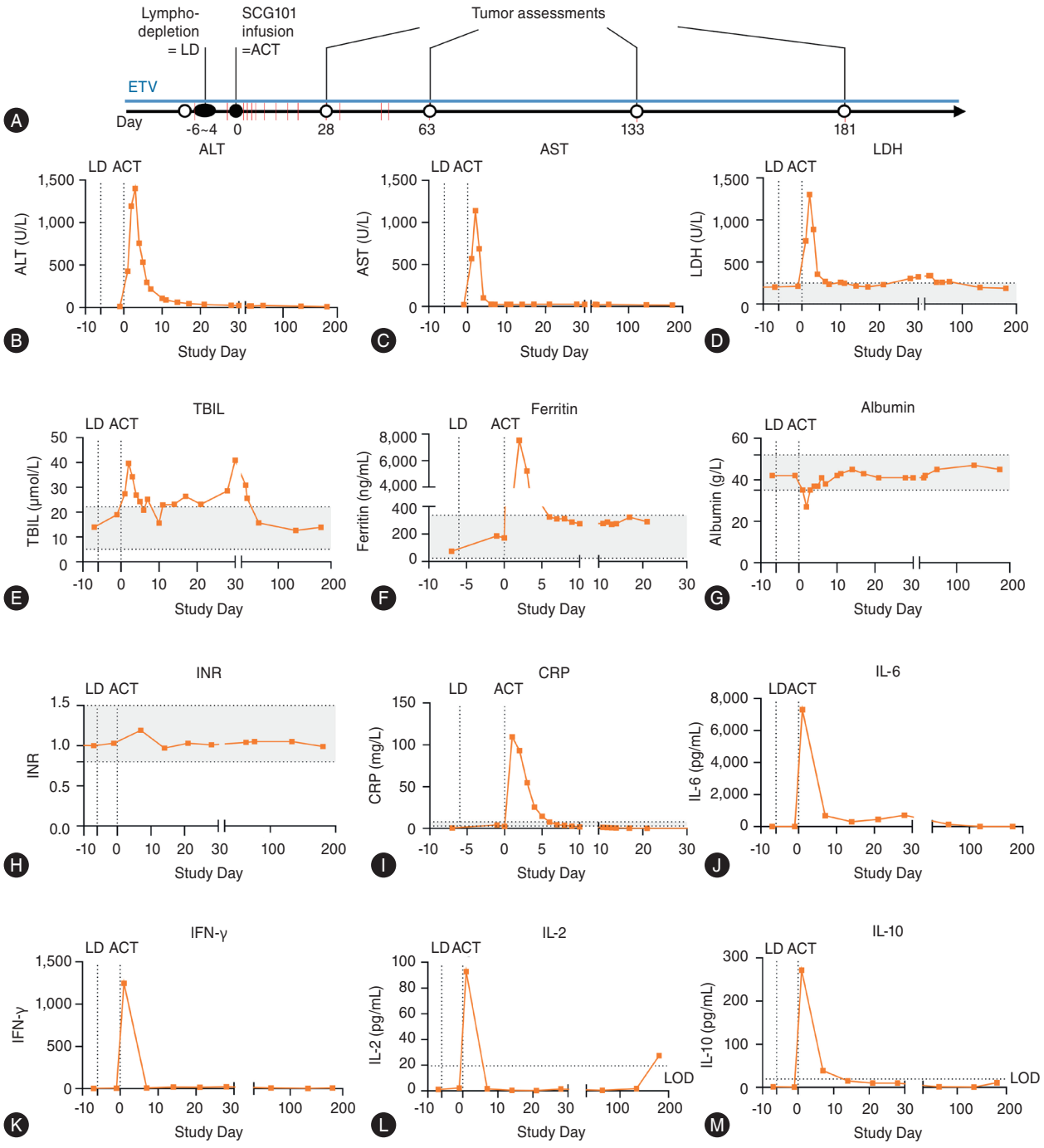

Figure 5. Liver and cytokine serum markers after transfer of HBV-specific SCG101 T cells. (A) Scheme of the drug administration (black circles) and tumor assessments (white circles). Following Cy/Flu lymphodepletion on days -6 to -4, a single dose of 7.9×10^7/kg (5.9×10^9 total) TCR-T cells was infused intravenously. Red lines indicate blood sample collections. (B–H) Serum markers of liver function, alanine transaminase (ALT), aspartate transaminase (AST), lactate dehydrogenase (LDH), TBIL (total bilirubin), ferritin, albumin, and the INR were measured on indicated days. A grey area indicates the normal range. (I) C-reactive protein (CRP) indicating ongoing inflammation. (J–M) Serum concentrations of IL-6, IFN-γ, IL-2, and IL-10 were determined by CBA. HBV, hepatitis B virus; Cy/Flu, cyclophosphamide plus fludarabine; TCR-T, T cell receptor T cells; LDH, lactate dehydrogenase; INR, international normalized ratio; IL, interleukin; IFN-γ, interferon-gamma; CBA, cytometric bead array; LOD, limit of detection; LD, lymphodepletion; ACT, adoptive cell transfer.

 https://doi.org/10.3350/cmh.2024.0058

Table 1. Treatment-related adverse events ≥grade 3

TRAE	Highest severity	Relation with SCG101	Other possible reasons	≥G3 AE duration
CRS	Grade 3	Definitely related	\	G3: D1-3
Hypotension	Grade 3	Possibly related	\	G3: D1-2
Decreased white blood cell count	Grade 4	Possibly related	Lymphodepletion	G4: D0-4 G3: D4-5, D14-17, D21-22, D28-30, 31-34
Decreased neutrophil count	Grade 4	Possibly related	Lymphodepletion	G4: D2-4, D28-30 G3: D0-2, 13-17, 31-34, 48-52
Decreased platelet count	Grade 4	Possibly related	Lymphodepletion	G4: D2-3, D4-6, D21-28 G3: D0-2, D3-4, D6-11, D12-13, D14-21
	Grade 3	Possibly related	Hepatocellular carcinoma	G3: D30-43, D77-80
Decreased lymphocyte count	Grade 3	Possibly related	Lymphodepletion	G3: D28-31
Increased ALT	Grade 4	Possibly related	Lymphodepletion	G4: D2-4 G3: D1-2, D4-7
Increased AST	Grade 4	Possibly related	Lymphodepletion	G4: D2-3 G3: D1-2, D3-4

All these ≥grade 3 were resolved or returned to baseline at the end of the AE.
TRAE, treatment related adverse event; G3, grade 3; G4, grade 4; CRS, cytokine release syndrome; ALT, alanine aminotransferase; AST, aspartate aminotransferase

peaking at 39.8°C (Supplementary Fig. 4L) and hypotension with a minimum blood pressure of 70/41 mmHg (Supplementary Fig. 4M). The symptoms stabilized after antipyretic and symptomatic treatment with norepinephrine and rehydration. Together, these symptoms indicated a CRS and were contained with Tocilizumab and dexamethasone (10 mg; 2x d1, 4x d2, 1x d3) and the subject started to recover by day three post-infusion. In summary, infusion of SCG101 induced non-serious side effects that were expected due to SCG101's mode of action and were manageable with standard medication for immune-related events.

Expansion of HBV-specific T cells in peripheral blood

The efficacy of adoptive T-cell therapy in both liquid and solid tumors using gene-modified T cells is associated with the persistence of transferred cells.[20,21] We, therefore, analyzed this by flow cytometry and qPCR. *Ex vivo*, transferred T cells at peak expansion constituted around one-third of $CD3^+$ T cells in blood detected by flow cytometry (Fig. 6A, Supplementary Fig. 5A) with a maximum of 4.37×10^4 cells/mL on day 21, suggesting a strong expansion (Fig. 6B). Both $CD8^+$ and $CD4^+$ HBV-specific TCR^+ T cells circulated equally indicating a slight increase in $CD4^+$ SCG101 T cells in blood compared to their proportion in the infusion product (Fig. 6B, Supplementary Fig. 3A, Supplementary Fig. 5B). Interestingly, while on day seven effector memory T cells ($CCR7^-CD45RA^-$) were still detected at equal numbers, mainly effector T cells ($CCR7^-CD45RA^+$) and T memory stem cells (T_{SCM}, $CCR7^+CD45RA^+$) circulated in peripheral blood thereafter within the first four weeks (Fig. 6C, Supplementary Fig. 5C). HBV-specific T cells were able to persist at least until four months post-transfer and by then almost exclusively consisted of T_{SCM} cells (Fig. 6C, Supplementary Fig. 5C). Long-term survival of transferred transduced T cells was confirmed by quantification of the copy number of the lentiviral vector integrates (Fig. 6D). This qPCR analysis indicated a peak in viral-vector copies seven days post-transfer, stabilizing until day 21 and slowly dropping thereafter. Collectively, these data demonstrated an enduring persistence of engineered T cells circulating in the blood associated with the development and maintenance of a predominantly stem cell memory phenotype after antigen exposure.

https://doi.org/10.3350/cmh.2024.0058

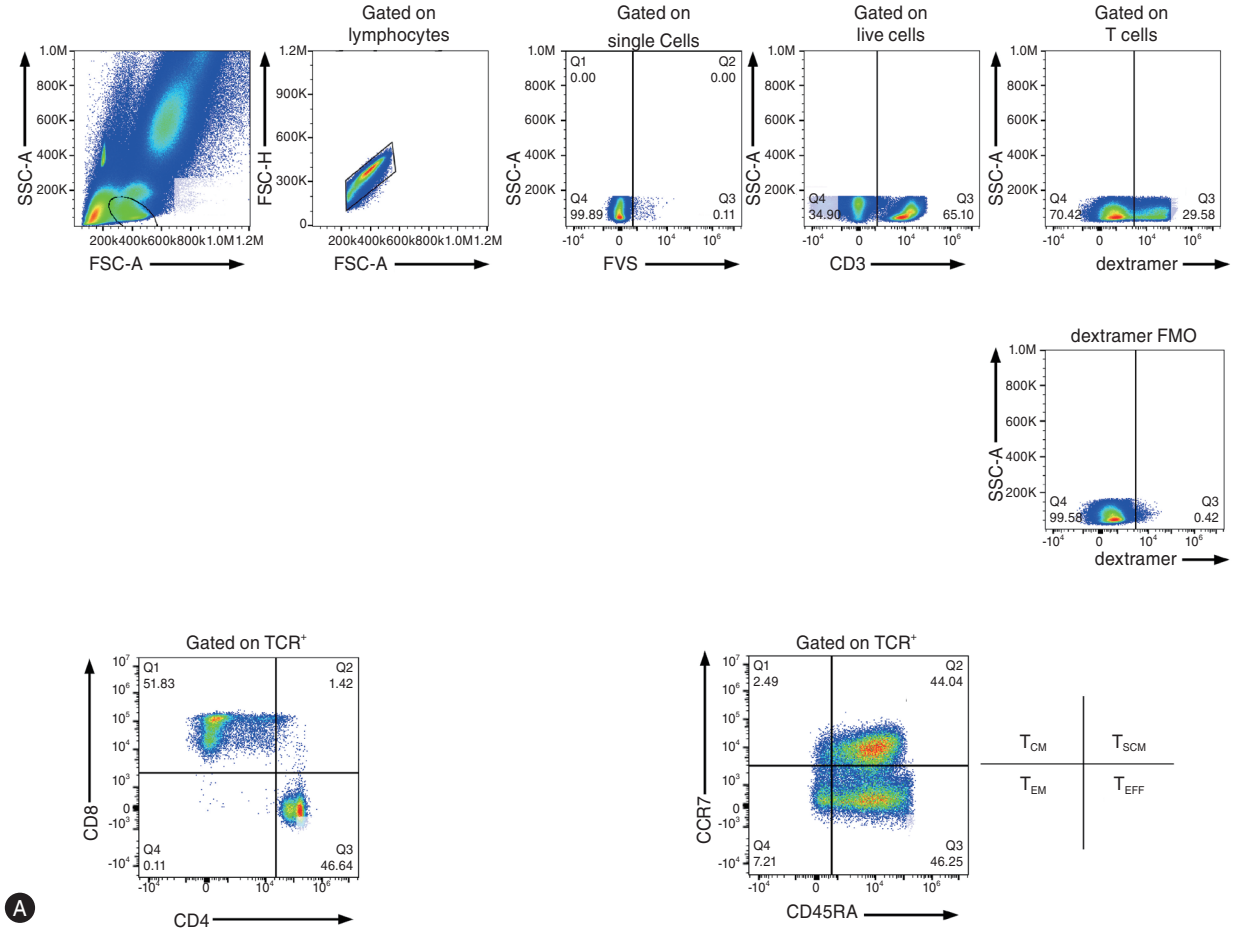

Figure 6. *Ex vivo* analysis of transferred T cells. (A) Flow cytometry gating strategy exemplified with a blood sample taken 21 days post-transfer. Single living lymphocytes were gated first, followed by identification of transferred cells via anti-CD3 and HBV S_{20}-dextramer staining. In two separate staining panels, dextramer-binding TCR^+ T cells were stained either for the T cell subsets with anti-CD8 and anti-CD4, or for memory differentiation status with anti-CCR7 and anti-CD45RA. Given the unspecific stimulation during T cell transduction and the antigen encounter after infusion, $CCR7^+$ $CD45RA^+$ cells were considered T_{SCM} and not naïve cells. The FMO (fluorescence minus one) control shows a staining without dextramer. (B, C) Flow cytometry analysis of blood samples taken after the cell transfer, gated on $CD3^+$ and HBV-S_{20}-$dextramer^+$ cells (blue circles). TCR^+ T cells stained either for the T-cell subsets with anti-CD8 (pink triangle) or anti-CD4 (purple triangle), or for memory differentiation status with anti-CCR7 and anti-CD45RA. T_{CM}:$CCR7^+CD45RA^-$ (red squares), T_{SCM}:$CCR7^+CD45RA^+$ (green triangle), T_{EM}:$CCR7^-CD45RA^-$ (black circles), T_{EFF}:$CCR7^-CD45RA^+$ (orange diamond). Different T-cell phenotypes were analyzed on indicated days and quantified using counting beads. (D) Genomic DNA was extracted from blood samples and the viral copy number (VCN) was quantified via qPCR. HBV, hepatitis B virus; TCR, T cell receptor; CCR, C-C chemokine receptor; qPCR, quantitative polymerase chain reaction.

Antiviral and antitumor activity of T cells redirected against HBsAg

Coinciding with the expansion of HBV-specific T cells and the increase in serum ALT, serum HBsAg substantially and rapidly decreased within one week after cell transfer from 557.96 to 1.3 IU/mL. The maximum reduction from baseline was 3.84 log_{10} to 0.08 IU/mL. It was maintained for more than six months (Fig. 7A). Serum HBV-DNA levels were low at baseline (29 IU/mL) and remained undetectable after cell infusion (Fig. 7B). Since no tumor tissue was contained in the biopsies obtained before treatment, the presence of the target on tumor cells remained unknown, and changes in HBsAg expression could only be analyzed in hepatocytes. Compared to the HBsAg expression in 10% of hepatocytes at screening (Fig. 4F), we barely observed HBsAg staining in hepatocytes by 73 days after cell infusion (Fig. 7C). Alpha-fetoprotein (AFP) levels fluctuated

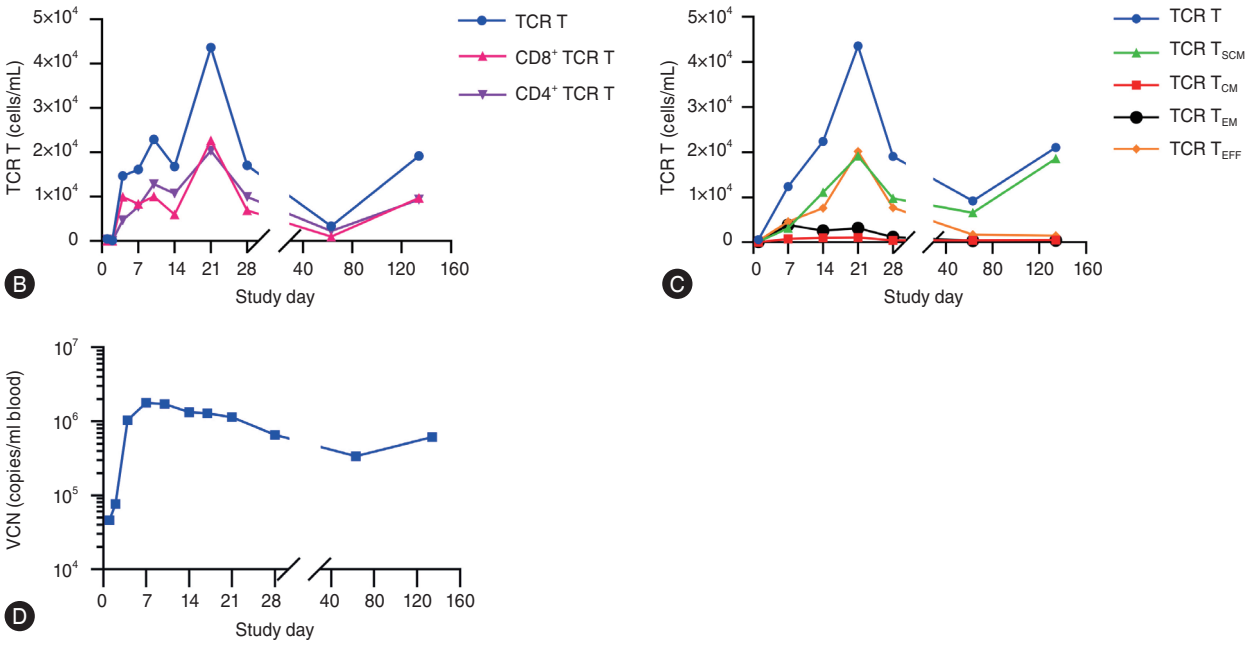

Figure 6. Continued.

and remained below 90 ng/mL until increasing again by day 133 (Supplementary Fig. 4N).

At baseline, the subject presented with multiple nodules and two target lesions in the right lobe with a 38- and 21-mm diameter, respectively (Fig. 7D, upper row). By day 28 post SCG101 infusion, a large area of tumor necrosis was observed (Fig. 7D, 2nd row), followed by a partial response with the target tumor lesions decreasing by 74.5% per mRECIST and by 47.5% per iRECIST, respectively. The patient maintained a stable disease for at least 6.9 months, suggesting clinical antiviral as well as antitumor activity of HBV-specific T cells.

DISCUSSION

HBV infection is a main driver for the development of HCC, and the available treatment options are limited. We here show that autologous, HBV-specific T cells can be manufactured using lentiviral transduction of a high-affinity TCR under GMP conditions, persist over several months, are safe and functioning in the clinical setting of an HBV-HCC, and lead to a profound reduction in viral markers and tumor mass.

SCG101 carries a natural TCR isolated from an HLA-A*02:01 donor with resolved HBV infection.[17] Hence, it had undergone negative selection against self-antigens within the thymus of the donor, and, not surprisingly, we did not observe any off-target activity in the patient. Although an alanine-substitution scan identified position five to be part of the TCR recognition motif, SCG101 was capable of recognizing the two most common HBV peptide variants FLLTRILTI (gtA,C,D) and FLLTKILTI (gtB). This cross-recognition could be explained by Arginine (R) and Lysine (K) as positively charged amino acids sharing more similar properties than Arginine and Alanine. Furthermore, preclinical toxicology and distribution studies were performed according to regulatory standards. However, these xenograft mouse models can only provide limited information since cytokines, chemokines, and receptors do not match between the human T-cell product and the murine recipient. Therefore, it is reassuring to know that T-cell transfer was also safe in a syngeneic mouse model when murine SCG101 T cells were injected into HBV$^+$HLA-A2$^+$ mice.[22]

Overall, the treatment was well-tolerated, all TRAEs were reversible through symptomatic interventions, and neither SAE nor dose-limiting toxicity (DLT) occurred. Grade 3 CRS became evident by an elevation of IL-6, fever, and hypotension, which likely led to increased levels of creatinine and urea in the blood due to reduced renal blood perfu-

https://doi.org/10.3350/cmh.2024.0058

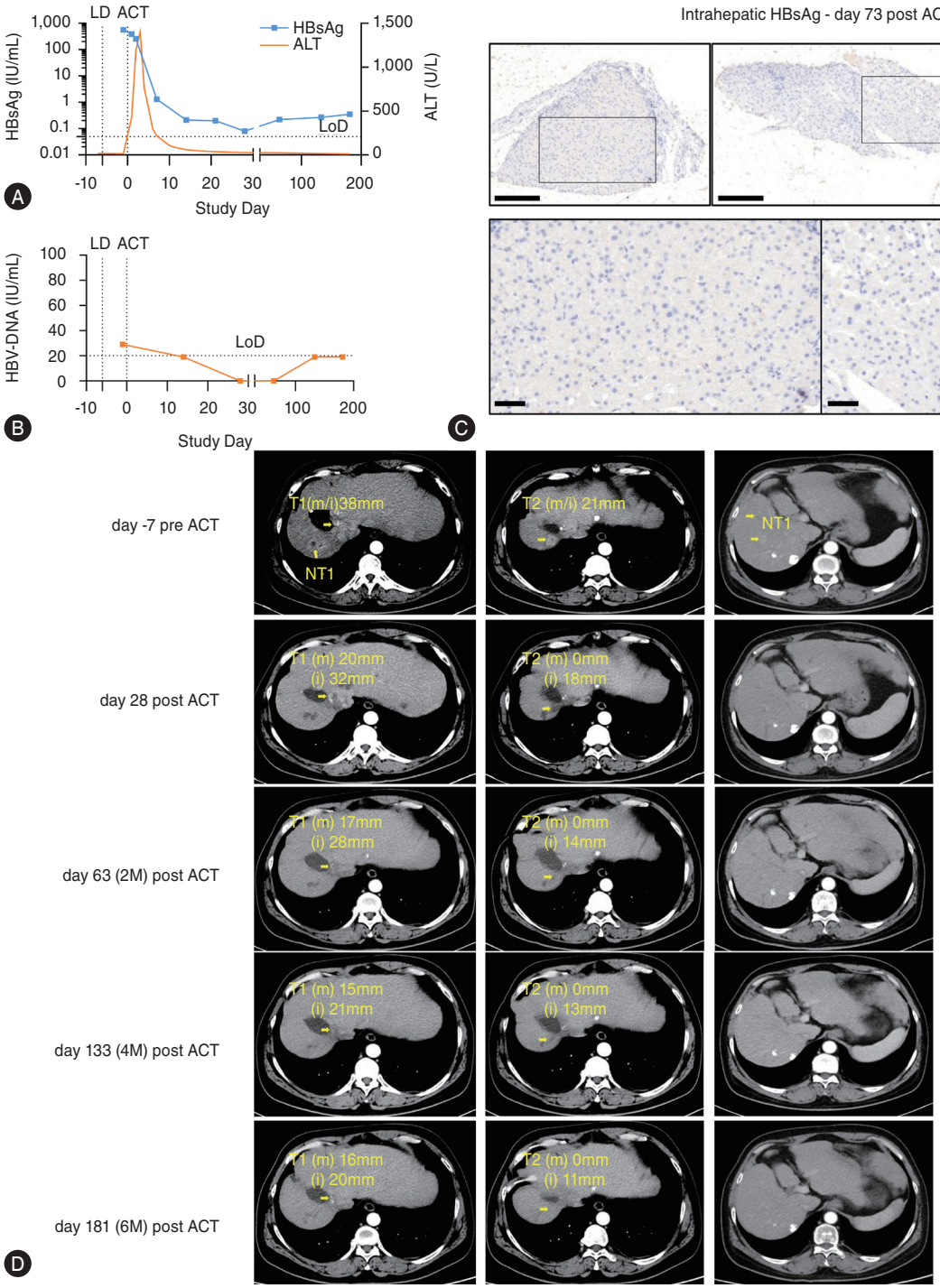

Figure 7. Antiviral and antitumor response after treatment with HBV-specific SCG101 T cells. (A) HBsAg (left axis, blue squares) was measured in serum at indicated time points. The diagnostic ELISA's lower limit of detection (LoD) was 0.05 IU/mL. ALT values (right axis, orange line) from Figure 6B were plotted again to better visually correlate both markers. The adoptive cell transfer (ACT) time point is indicated with a dashed line. (B) HBV-DNA was measured in sera via qPCR. (C) Immunostaining of HBsAg of a liver biopsy taken 73 days after treatment. One piece of non-tumor liver tissue was obtained. Scale bars: 200 μm and 50 μm (inlay), respectively. (D) The tumor burden was analyzed via multiphasic CT scan on days -7 prior to treatment and on days 28, 63, 133, and 181 after ACT. The size of the target (T) lesion no.1 and no.2 in mRECIST (m) or iRECIST (i) and the position of non-target (NT) lesions are indicated in yellow. HBV, hepatitis B virus; HBsAg, hepatitis B surface antigen; ALT, alanine aminotransferase; qPCR, quantitative polymerase chain reaction; CT, computer-assisted tomography.

https://doi.org/10.3350/cmh.2024.0058

sion. CRS was effectively managed with tocilizumab, corticoids, and noradrenaline. Notably, in the treatment of CD19-malignancies, CRS typically occurs more than 24 hours after CAR-T-cell infusion.[23] However, in the case presented here, the onset of CRS was unexpectedly rapid, with elevated body temperature and high IL-6 levels observed as early as two hours after the infusion. Generally, it is assumed that IIFN-γ released by activated T cells leads to IL-6 production in bystander cells such as macrophages.[24] Our *in vitro* experiments using real-time cytotoxicity measurement revealed that T-cell activation and target cell killing occurred immediately after the co-culture began. Potentially, in the patient, effector function of the T cells started immediately after infiltration into the tissue, and the significant number of liver-resident Kupffer cell macrophages may have contributed to the rapid onset of CRS.

All grade 4 events (cytopenia and increased ALT/AST levels) were expected to be a positive sign of response to treatment. Cytopenia was intended and most likely induced by the pre-conditioning Cy/Flu regimen, which has been associated with better T-cell engraftment and outcome in CD19 CAR-T treatment.[25] The reasons why patients benefit from lymphodepletion prior to ACT are not fully understood, and co-depletion of regulatory cells,[26] an increase of serum cytokines,[27,28] and tolerization towards xenogeneic sequences[29] have been discussed. Cytopenia also comprised a low platelet count, which started already at screening before treatment. It might have been prolonged due to multiple factors, including lymphodepletion, tocilizumab treatment, and the study drug's proliferation. We suppose that a more proactive use of recombinant human thrombopoietin or thrombopoietin receptor agonists can be considered to help the platelet count recover under such circumstances.

The elevation in ALT/AST levels occurred concomitantly with a substantial reduction in serum HBsAg and is in line with SCG101's anti-tumor and anti-viral cytotoxicity demonstrated before.[18] Notably, in addition to targeting tumor cells, HBV-specific T cells also recognize and attack hepatocytes that express HBsAg or fragments thereof, either due to HBV infection or HBV-DNA integration,[18] which likely led to the transient increase in serum transaminases. The ALT levels in our patient reached 35-fold the ULN. This, however, did not result in hepatic dysfunction or severe hepatic damage as evidenced by the absence of impaired liver synthetic function (bilirubin, albumin, or INR), the absence of specific symptoms such as jaundice or bleeding, and the transient nature of the flare.[30] Cytotoxicity directed towards non-tumor HBV$^+$ hepatocytes is inherently linked to an effective T-cell response, either naturally generated during acute hepatitis and viral clearance or artificially generated via transfer of immune cells.[31] Indeed, transient ALT flares that are host-induced, i.e., comprising an effective immune response, but not virus-induced, can be associated with favorable outcomes[30] and viral clearance.[32,33]

Nonetheless, the mitigation of excessive liver damage following adoptive T-cell transfer remains a priority. To address this, inclusion required a Child-Pugh score ≤7 and ECOG performance status of 0 or 1 as well, and pre-treatment biopsies were analyzed for HBsAg$^+$ hepatocytes. Several studies have examined CHB patient biopsies to determine the frequency of HBsAg$^+$ hepatocytes with high variation from 0% to 100%,[34-39] with particularly high levels when ground glass hepatocytes are present.[37] The most recent and comprehensive study by Aggarwal et al. analyzed biopsies from 114 patients, finding the average proportion of HBsAg$^+$ hepatocytes to be below 10%. Interestingly, they observed a lack of correlation between quantification results from two biopsies collected from the same individual and time point.[36] This aligns with our findings of heterogenic HBsAg staining for subject ST1206, suggesting that multiple biopsies may be necessary to yield reliable results representing the entire liver. This information could be complemented by serum HBsAg levels, which generally, though not always,[34] correlate with intrahepatic HBsAg levels.[40] Additionally, more sophisticated probe-[13] or sequencing-based[41] assays might be necessary to assess the presence of the target peptide expressed from chimeras of HBV and host-cell nucleic acids that might not cover the full HBsAg open reading frame and might not be detectable by antibody staining.[13] We anticipate insights from the ongoing phase I/II study of SCG101 (NCT05417932) will contribute to identifying a reliable biomarker for safe patient stratification.

The patient described here was negative for HBcAg liver staining, HBeAg, and HBV-DNA, leading to the assumption that most of the serum HBsAg originated from tumor cells and/or hepatocytes with HBV-DNA integration rather than from active infection. Studies have indicated that HBsAg and HBcAg rarely colocalize in biopsy samples[9,36] and that in late-stage CHB, integrated HBV-DNA is the main source

https://doi.org/10.3350/cmh.2024.0058

for HBsAg production.[42-44] HBsAg decline is the hallmark of effective anti-HBV treatment[45] and has not been achieved by RNA-interference-based therapies,[46] likely due to integrated HBV-DNA being the source of HBsAg.[47] Therefore, targeting integrated HBV-DNA has been suggested to be a goal in drug development.[48,49] With SCG101 treatment, we observed a considerable reduction in HBsAg, approaching the detection limit of the diagnostic assay, which would have constituted a functional cure. Over six months, HBsAg levels did not rebound but were also not eliminated despite SCG101 persistence, and several reasons for this observation can be discussed. First, it is possible that HBsAg$^+$ cells developed evasion strategies, such as HLA-loss or mutations in the peptide presentation pathway, similar to what has been observed in HPV-cancer patients refractory to treatment with HPV-specific T cells.[50] Second, SCG101 cells might have undergone similar exhaustion mechanisms as endogenous HBV-specific T cells in the liver and tumor.[51,52] Due to the limited amount of blood available for analysis, we were unfortunately unable to address this hypothesis. Although SCG101 T cells were still circulating in the blood after several months, we have no proof that they retained their functionality. However, in mice transduced with AAV-HBV and AAV-HLA-A2, we observed the same kinetics of ALT increase, HBsAg reduction, and persistence of HBV-specific T cells. Also, a residual low amount of HBsAg remained detectable in this syngeneic mouse model. When T cells were analyzed *ex vivo*, the high-avidity TCR-T cells could no longer be specifically activated by their cognate peptide.[22]

Most importantly, following activation of SCG101 in subject ST1206, a sizable and sustained antitumor effect was observed 28 days after cell infusion, lasting at least until the cut-off date. While tumor shrinkage occurred directly after SCG101 infusion, without a pre-treatment tumor biopsy, we can only speculate but not prove its direct cytotoxicity on tumor cells. Alternatively, an indirect effect can be envisioned, where SCG101 cells create an inflammatory environment, helping endogenous immune cells attack the tumor. This idea was already proposed when two patients treated with RNA-electroporated TCR-T cells experienced clear shrinkage of the primary tumor[53,54] or metastases.[13] Using mRNA, anti-tumor responses occurred only after several infusions and during a time frame when the transferred cells most likely had lost their designed antigen-specificity due to the transient HBV-TCR expression after mRNA electroporation, while still other immunological alterations were detected.[13,54]

Notably, four months after T-cell infusion, a moderate rise in AFP levels was observed in our patient, exceeding pre-infusion levels. This AFP increase could indicate liver regeneration, as similar AFP rises have been observed in acute hepatitis B and correlated positively with the extent of transaminase elevation.[55,56] However, in this study, peak transaminase levels were followed by the AFP increase only four weeks later. Another potential hypothesis for the increase in AFP is that eliminating HBsAg$^+$ tumor and pre-malignant cells created space for HCC cells negative for the S_{20} target peptide of SCG101 to proliferate. Mason et al.[6] proposed the "loss of productive HBV infection, providing at least partial escape from the antiviral immune response as a major facilitator of clonal expansion". Given the early emergence of clonal growth,[5] we would expect this postulated negative effect of an antiviral immune response to also manifest in an increased number of HCC cases after spontaneous clearance in late-stage CHB. However, further investigations in larger cohorts are required to gather more data on this phenomenon.

The on-target efficacy observed with our selected dose of SCG101 and treatment scheme exceeded similar - albeit different - regimens using HBV-specific T cells transiently expressing a TCR after electroporation.[13,53] In patients with the indication of HBV-HCC-derived metastases and an HLA-A2 negative and/or HBV-negative liver after transplantation.[13,57] HBsAg was reduced by almost 50% in 2/8 patients three to six months after infusing several doses of transient, RNA-electroporated TCR T cells[53] or by 90% in a single patient one month after infusion of stably transduced TCR-T cells.[57] Although it is difficult to quantitatively compare these approaches due to different clinical settings, cell doses and duration of cellular functionality, it was remarkable that in the pioneering study of Qasim et al.[57], the stably transduced TCR-T seemed to act faster and more efficiently despite a low transduction rate and a low dose of cells infused.

This encouraged us to set up a highly efficient GMP-compliant transduction process generating higher TCR-T numbers that - as demonstrated in this study - after infusion quickly reduced HBsAg by 99.99%. Along with the stable expression of the TCR, other factors might have

contributed to the clinical efficacy of SCG101. Its dual functionality in $CD8^+$ and $CD4^+$ T cells, the balance of both T-cell subtypes, and the shift to a memory stem cell phenotype might have supported the persistence and extended functionality of transferred T cells. A well-balanced CD8:CD4 T-cell ratio and the occurrence of the T_{SCM} phenotype have positively impacted the outcome of CAR-T therapy.[58-60] Potentially, also the encounter of HBsAg on hepatocytes may have facilitated the stimulation and expansion of transferred, stably TCR-expressing T cells before encountering the immunosuppressive tumor microenvironment. Others currently follow the same principle of using an RNA-vaccine to boost transferred claudin-specific CAR T cells to treat solid tumors.[61]

Overall, SCG101 was shown to be a safe product with its stable TCR expression, leading to both antitumor and antiviral effector functions and sustained persistence in the patient. Further studies will determine whether adoptive T-cell therapy can maintain a favorable risk-benefit ratio and has the potential to be applied to target the cause of malignant transformation to prevent additional tumor development.

Authors' contribution

TJ and LY prepared preclinical experiments; SD and CM designed the clinical study; XuWa, XiWu, FL, and YW performed T-cell transfer and follow-up treatment; KW, XiWa, YP and QL analyzed data; KW wrote the manuscript; KZ, UP, and SD interpreted data and critically revised the manuscript.

Acknowledgements

This study was supported by SCG Cell Therapy Pte. Ltd., and the Deutsche Forschungsgemeinschaft (DFG, German Research Foundation) via SFB-TRR 338/1 2021–452881907 to UP.

Conflicts of Interest

KW, TJ, LY, XiWa, YP, QL, CM and KZ are employees of SCG Cell Therapy; KZ and UP are board members of SCG Cell Therapy; KW, KZ, CM, and UP hold shares in SCG Cell Therapy Pte. Ltd. KW, TJ, KZ and UP have a patent WO2023239290 pending. UP receives research funding from SCG Cell Therapy. The other authors declare no conflict of interest.

SUPPLEMENTARY MATERIAL

Supplementary material is available at Clinical and Molecular Hepatology website (http://www.e-cmh.org).

REFERENCES

1. Sung H, Ferlay J, Siegel RL, Laversanne M, Soerjomataram I, Jemal A, et al Global cancer statistics 2020: GLOBOCAN estimates of incidence and mortality worldwide for 36 cancers in 185 Countries. CA Cancer J Clin 2021;71:209-249.
2. Zhang H, Zhang W, Jiang L, Chen Y. Recent advances in systemic therapy for hepatocellular carcinoma. Biomark Res 2022;10:3.
3. Zheng R, Qu C, Zhang S, Zeng H, Sun K, Gu X, et al. Liver cancer incidence and mortality in China: Temporal trends and projections to 2030. Chin J Cancer Res 2018;30:571-579.
4. Sung WK, Zheng H, Li S, Chen R, Liu X, Li Y, et al. Genome-wide survey of recurrent HBV integration in hepatocellular carcinoma. Nat Genet 2012;44:765-769.
5. Tu T, Mason WS, Clouston AD, Shackel NA, McCaughan GW, Yeh MM, et al. Clonal expansion of hepatocytes with a selective advantage occurs during all stages of chronic hepatitis B virus infection. J Viral Hepat 2015;22:737-753.
6. Mason WS, Jilbert AR, Litwin S. Hepatitis B virus DNA integration and clonal expansion of hepatocytes in the chronically infected liver. Viruses 2021;13:210.
7. Ringlander J, Skoglund C, Prakash K, Andersson ME, Larsson SB, Tang KW, et al. Deep sequencing of liver explant transcriptomes reveals extensive expression from integrated hepatitis B virus DNA. J Viral Hepat 2020;27:1162-1176.
8. Su IJ, Wang HC, Wu HC, Huang WY. Ground glass hepatocytes contain pre-S mutants and represent preneoplastic lesions in chronic hepatitis B virus infection. J Gastroenterol Hepatol 2008;23:1169-1174.
9. Zheng Y, Xu M, Zeng D, Tong H, Shi Y, Feng Y, et al. In situ analysis of hepatitis B virus (HBV) antigen and DNA in HBV-induced hepatocellular carcinoma. Diagn Pathol 2022;17:11.
10. Wang Y, Wu MC, Sham JS, Tai LS, Fang Y, Wu WQ, et al. Different expression of hepatitis B surface antigen between hepatocellular carcinoma and its surrounding liver tissue, studied using a tissue microarray. J Pathol 2002;197:610-616.
11. Tantiwetrueangdet A, Panvichian R, Sornmayura P, Suean-

goen N, Leelaudomlipi S. Reduced HBV cccDNA and HBsAg in HBV-associated hepatocellular carcinoma tissues. Med Oncol 2018;35:127.
12. Fu S, Li N, Zhou PC, Huang Y, Zhou RR, Fan XG. Detection of HBV DNA and antigens in HBsAg-positive patients with primary hepatocellular carcinoma. Clin Res Hepatol Gastroenterol 2017;41:415-423.
13. Tan AT, Yang N, Lee Krishnamoorthy T, Oei V, Chua A, Zhao X, et al. Use of expression profiles of HBV-DNA integrated into genomes of hepatocellular carcinoma cells to select T cells for immunotherapy. Gastroenterology 2019;156:1862-1876.e9.
14. Srivastava M, Copin R, Choy A, Zhou A, Olsen O, Wolf S, et al. Proteogenomic identification of Hepatitis B virus (HBV) genotype-specific HLA-I restricted peptides from HBV-positive patient liver tissues. Front Immunol 2022;13:1032716.
15. de Beijer MTA, Bezstarosti K, Luijten R, Doff WAS, Boor PPC, Pieterman RFA, et al. Immunopeptidome of hepatocytes isolated from patients with HBV infection and hepatocellular carcinoma. JHEP Rep 2022;4:100576.
16. Gehring AJ, Xue SA, Ho ZZ, Teoh D, Ruedl C, Chia A, et al. Engineering virus-specific T cells that target HBV infected hepatocytes and hepatocellular carcinoma cell lines. J Hepatol 2011;55:103-110.
17. Wisskirchen K, Metzger K, Schreiber S, Asen T, Weigand L, Dargel C, et al. Isolation and functional characterization of hepatitis B virus-specific T-cell receptors as new tools for experimental and clinical use. PLoS One 2017;12:e0182936.
18. Wisskirchen K, Kah J, Malo A, Asen T, Volz T, Allweiss L, et al. T cell receptor grafting allows virological control of Hepatitis B virus infection. J Clin Invest 2019;129:2932-2945.
19. Sommermeyer D, Uckert W. Minimal amino acid exchange in human TCR constant regions fosters improved function of TCR gene-modified T cells. J Immunol 2010;184:6223-6231.
20. Porter DL, Hwang WT, Frey NV, Lacey SF, Shaw PA, Loren AW, et al. Chimeric antigen receptor T cells persist and induce sustained remissions in relapsed refractory chronic lymphocytic leukemia. Sci Transl Med 2015;7:303ra139.
21. Louis CU, Savoldo B, Dotti G, Pule M, Yvon E, Myers GD, et al. Antitumor activity and long-term fate of chimeric antigen receptor-positive T cells in patients with neuroblastoma. Blood 2011;118:6050-6056.
22. Festag J, Festag MM, Asen T, Wettengel JM, Mück-Häusl MA, Abdulhaqq S, et al. Vector-mediated delivery of human major histocompatibility complex-I into hepatocytes enables investigation of T cell receptor-redirected hepatitis B virus-specific T cells in mice, and in macaque cell cultures. Hum Gene Ther 2023;34:1204-1218.
23. Lee DW, Santomasso BD, Locke FL, Ghobadi A, Turtle CJ, Brudno JN, et al. ASTCT Consensus grading for cytokine release syndrome and neurologic toxicity associated with immune effector cells. Biol Blood Marrow Transplant 2019;25:625-638.
24. Shimabukuro-Vornhagen A, Gödel P, Subklewe M, Stemmler HJ, Schlößer HA, Schlaak M, et al. Cytokine release syndrome. J Immunother Cancer 2018;6:56.
25. Turtle CJ, Hanafi LA, Berger C, Gooley TA, Cherian S, Hudecek M, et al. CD19 CAR-T cells of defined CD4+:CD8+ composition in adult B cell ALL patients. J Clin Invest 2016;126:2123-2138.
26. Muranski P, Boni A, Wrzesinski C, Citrin DE, Rosenberg SA, Childs R, et al. Increased intensity lymphodepletion and adoptive immunotherapy--how far can we go? Nat Clin Pract Oncol 2006;3:668-681.
27. Kielsen K, Oostenbrink LVE, von Asmuth EGJ, Jansen-Hoogendijk AM, van Ostaijen-Ten Dam MM, Ifversen M, et al. IL-7 and IL-15 levels reflect the degree of T cell depletion during lymphopenia and are associated with an expansion of effector memory T cells after pediatric hematopoietic stem cell transplantation. J Immunol 2021;206:2828-2838.
28. Heczey A, Louis CU, Savoldo B, Dakhova O, Durett A, Grilley B, et al. CAR T cells administered in combination with lymphodepletion and PD-1 inhibition to patients with neuroblastoma. Mol Ther 2017;25:2214-2224.
29. Festag MM, Festag J, Fräßle SP, Asen T, Sacherl J, Schreiber S, et al. Evaluation of a fully human, hepatitis B virus-specific chimeric antigen receptor in an immunocompetent mouse model. Mol Ther 2019;27:947-959.
30. European Association for the Study of the Liver. EASL 2017 Clinical Practice Guidelines on the management of hepatitis B virus infection. J Hepatol 2017;67:370-398.
31. Shouval D. Adoptive transfer of immunity to HBV in liver transplant patients: a step forward toward the proof of concept for therapeutic vaccination or a transient immunologic phenomenon? Liver Transpl 2007;13:14-17.
32. Sonneveld MJ, Zoutendijk R, Flink HJ, Zwang L, Hansen BE, Janssen HL. Close monitoring of hepatitis B surface antigen levels helps classify flares during peginterferon therapy and predicts treatment response. Clin Infect Dis 2013;56:100-105.
33. Chi H, Arends P, Reijnders JG, Carey I, Brown A, Fasano M, et al. Flares during long-term entecavir therapy in chronic hepati-

tis B. J Gastroenterol Hepatol 2016;31:1882-1887.
34. Montanari NR, Ramírez R, Aggarwal A, van Buuren N, Doukas M, Moon C, et al. Multi-parametric analysis of human livers reveals variation in intrahepatic inflammation across phases of chronic hepatitis B infection. J Hepatol 2022;77:332-343.
35. Meier MA, Calabrese D, Suslov A, Terracciano LM, Heim MH, Wieland S. Ubiquitous expression of HBsAg from integrated HBV DNA in patients with low viral load. J Hepatol 2021;75:840-847.
36. Aggarwal A, Odorizzi PM, Brodbeck J, van Buuren N, Moon C, Chang S, et al. Intrahepatic quantification of HBV antigens in chronic hepatitis B reveals heterogeneity and treatment-mediated reductions in HBV core-positive cells. JHEP Rep 2022;5:100664.
37. Cheng PN, Chiu YC, Tsai HW, Wang RH, Chiu HC, Wu IC, et al. HBsAg expression of liver correlates with histological activities and viral replication in chronic hepatitis B. Ann Hepatol 2014;13:771-780.
38. Chu CM, Liaw YF. Membrane staining for hepatitis B surface antigen on hepatocytes: a sensitive and specific marker of active viral replication in hepatitis B. J Clin Pathol 1995;48:470-473.
39. Wursthorn K, Lutgehetmann M, Dandri M, Volz T, Buggisch P, Zollner B, et al. Peginterferon alpha-2b plus adefovir induce strong cccDNA decline and HBsAg reduction in patients with chronic hepatitis B. Hepatology 2006;44:675-684.
40. Thompson AJ, Nguyen T, Iser D, Ayres A, Jackson K, Littlejohn M, et al. Serum hepatitis B surface antigen and hepatitis B e antigen titers: disease phase influences correlation with viral load and intrahepatic hepatitis B virus markers. Hepatology 2010;51:1933-1944.
41. Chen W, Zhang K, Dong P, Fanning G, Tao C, Zhang H, et al. Noninvasive chimeric DNA profiling identifies tumor-originated HBV integrants contributing to viral antigen expression in liver cancer. Hepatol Int 2020;14:326-337.
42. Svicher V, Salpini R, Piermatteo L, Carioti L, Battisti A, Colagrossi L, et al. Whole exome HBV DNA integration is independent of the intrahepatic HBV reservoir in HBeAg-negative chronic hepatitis B. Gut 2021;70:2337-2348.
43. Rydell GE, Larsson SB, Prakash K, Andersson M, Norder H, Hellstrand K, et al. Abundance of noncircular intrahepatic hepatitis B virus DNA may reflect frequent integration into human DNA in chronically infected patients. J Infect Dis 2022;225:1982-1990.
44. Grudda T, Hwang HS, Taddese M, Quinn J, Sulkowski MS, Sterling RK, et al. Integrated hepatitis B virus DNA maintains surface antigen production during antiviral treatment. J Clin Invest 2022;132:e161818.
45. Revill P, Testoni B, Locarnini S, Zoulim F. Global strategies are required to cure and eliminate HBV infection. Nat Rev Gastroenterol Hepatol 2016;13:239-248.
46. Yuen MF, Schiefke I, Yoon JH, Ahn SH, Heo J, Kim JH, et al. RNA interference therapy with ARC-520 results in prolonged hepatitis B surface antigen response in patients with chronic hepatitis B infection. Hepatology 2020;72:19-31.
47. Wooddell CI, Yuen MF, Chan HL, Gish RG, Locarnini SA, Chavez D, et al. RNAi-based treatment of chronically infected patients and chimpanzees reveals that integrated hepatitis B virus DNA is a source of HBsAg. Sci Transl Med 2017;9:eaan0241.
48. Wooddell CI, Gehring AJ, Yuen MF, Given BD. RNA interference therapy for chronic hepatitis B predicts the importance of addressing viral integration when developing novel cure strategies. Viruses 2021;13:581.
49. Cornberg M, Manns MP. Hepatitis: No cure for hepatitis B and D without targeting integrated viral DNA? Nat Rev Gastroenterol Hepatol 2018;15:195-196.
50. Nagarsheth NB, Norberg SM, Sinkoe AL, Adhikary S, Meyer TJ, Lack JB, et al. TCR-engineered T cells targeting E7 for patients with metastatic HPV-associated epithelial cancers. Nat Med 2021;27:419-425.
51. Baudi I, Kawashima K, Isogawa M. HBV-specific CD8+ T-cell tolerance in the liver. Front Immunol 2021;12:721975.
52. You M, Gao Y, Fu J, Xie R, Zhu Z, Hong Z, et al. Epigenetic regulation of HBV-specific tumor-infiltrating T cells in HBV-related HCC. Hepatology 2023;78:943-958.
53. Meng F, Zhao J, Tan AT, Hu W, Wang SY, Jin J, et al. Immunotherapy of HBV-related advanced hepatocellular carcinoma with short-term HBV-specific TCR expressed T cells: results of dose escalation, phase I trial. Hepatol Int 2021;15:1402-1412.
54. Tan AT, Meng F, Jin J, Zhang JY, Wang SY, Shi L, et al. Immunological alterations after immunotherapy with short lived HBV-TCR T cells associates with long-term treatment response in HBV-HCC. Hepatol Commun 2022;6:841-854.
55. Silver HK, Deneault J, Gold P, Thompson WG, Shuster J, Freedman SO. The detection of alpha 1-fetoprotein in patients with viral hepatitis. Cancer Res 1974;34:244-247.
56. Hanif H, Ali MJ, Susheela AT, Khan IW, Luna-Cuadros MA, Khan MM, et al. Update on the applications and limitations of alpha-fetoprotein for hepatocellular carcinoma. World J Gas-

troenterol 2022;28:216-229.
57. Qasim W, Brunetto M, Gehring AJ, Xue SA, Schurich A, Khakpoor A, et al. Immunotherapy of HCC metastases with autologous T cell receptor redirected T cells, targeting HBsAg in a liver transplant patient. J Hepatol 2015;62:486-491.
58. Sommermeyer D, Hudecek M, Kosasih PL, Gogishvili T, Maloney DG, Turtle CJ, et al. Chimeric antigen receptor-modified T cells derived from defined CD8+ and CD4+ subsets confer superior antitumor reactivity in vivo. Leukemia 2016;30:492-500.
59. Li Y, Wu D, Yang X, Zhou S. Immunotherapeutic potential of T memory stem cells. Front Oncol 2021;11:723888.
60. Biasco L, Izotova N, Rivat C, Ghorashian S, Richardson R, Guvenel A, et al. Clonal expansion of T memory stem cells determines early anti-leukemic responses and long-term CAR T cell persistence in patients. Nat Cancer 2021;2:629-642.
61. Reinhard K, Rengstl B, Oehm P, Michel K, Billmeier A, Hayduk N, et al. An RNA vaccine drives expansion and efficacy of claudin-CAR-T cells against solid tumors. Science 2020;367:446-453.